Available online at www.sciencedirect.com
ScienceDirect
Journal of Structural Biology 156 (2006) 355–362
Journal of Structural Biology
www.elsevier.com/locate/yjsbi

Microstructure and crystallographic-texture of giant barnacle (*Austromegabalanus psittacus*) shell

Alejandro B. Rodríguez-Navarro [a,*], Christiane CabraldeMelo [b], Nelson Batista [c], Nilton Morimoto [b], Pedro Alvarez-Lloret [a], Miguel Ortega-Huertas [a], Victor M. Fuenzalida [d], Jose I. Arias [d], Juan P. Wiff [d], Jose L. Arias [d,*]

[a] *Departamento de Mineralogía y Petrología, Universidad de Granada, Spain*
[b] *Escola Politécnica, LSI, Universidade de São Paulo, Brazil*
[c] *Instituto de Pesquisas Energéticas e Nucleares (IPEN), Centro de Ciencia e Tecnología de Materiais, São Paulo, Brazil*
[d] *Facultades de Ciencias Físicas y Matemáticas, y de Ciencias Veterinarias y Pecuarias, Universidad de Chile and CIMAT, Santiago, Chile*

Received 3 February 2006; received in revised form 26 April 2006; accepted 28 April 2006
Available online 7 May 2006

Abstract

Barnacle shell is a very complex and strong composite bioceramic composed of different structural units which consist of calcite 15 microcrystals of very uniform size. In the study reported herein, the microstructural organization of these units has been examinated in detail with optical and scanning electron microscopy, and X-ray diffraction techniques. These analyses showed that the external part of the shell has a massive microstructure consisting of randomly oriented crystals. Toward the interior, the shell became organized in mineral layers separated by thin organic sheets. Each of these mineral layers has a massive microstructure constituted by highly oriented calcite microcrystals with their *c*-axes aligned [(001) fibre texture] perpendicular to the organic sheets and the shell surface. Interestingly, in another structural unit, the shell shield, the orientation of the *c*-axis calcite crystals shifts from being perpendicular to being parallel to the shell surface across its thickness. This study provides evidence that the organic matrix is responsible for the organization of the shell mineral and exterts strong a strict control on the polymorphic type, size and orientation of shell-forming crystals.

Keywords: Biomineralization; Calcite; Organic matrix; Pole figures; XRD; X-ray diffraction; Crystallite size

1. Introduction

Austromegabalanus psittacus is a large (normally up to 30 cm high) sessile balanomorph barnacle from the coast of Chile and South Perú. Its mineralized shell is composed of calcite ($CaCO_3$) (Fernandez et al., 2001a,b; Arias, 2002). The shells consists of several structural components including twelve side plates, síx parietes, and síx radii which are cemented forming a truncated cone opened at the top (Fig. 1). The cone-shaped shell stands on a basal disk firmly cemented to the substratum to which the barnacle is attached. The conical aperture is partially obstructed by six oblique mineralized structures, referred as to the shell shield. Each of the components constituting the shell has different microstructural and crystallographic characteristics which will be described in detail in this study.

Shell mineral is deposited by mantle epithelial cells of the crustracean body which are in contact with the inner shell surface. The epithelial cells supply Ca^{2+} and HCO_3^- ions, which are necessary for the precipitation of calcium carbonate, and also supply specific organic components which regulate crystal growth. This is similar to the way mollusks mineralize their shel, although mollusks deposit their shell continuously (Nousek, 1984; Lowenstam and Weiner, 1989). In contrast, crustraceans grow by shedding their exoskeleton every molting cycle and depositing a new exoskeleton, which later mineralizes. Although they are crustraceans, barnacles only deminerlize and shed part

* Corresponding authors. Fax: +34 958243368.
E-mail address: anava@ugr.es (A.B. Rodríguez-Navarro).

1047-8477/$ - see front matter © 2006 Elsevier Inc. All rights reserved.
doi:10.1016/j.jsb.2006.04.009

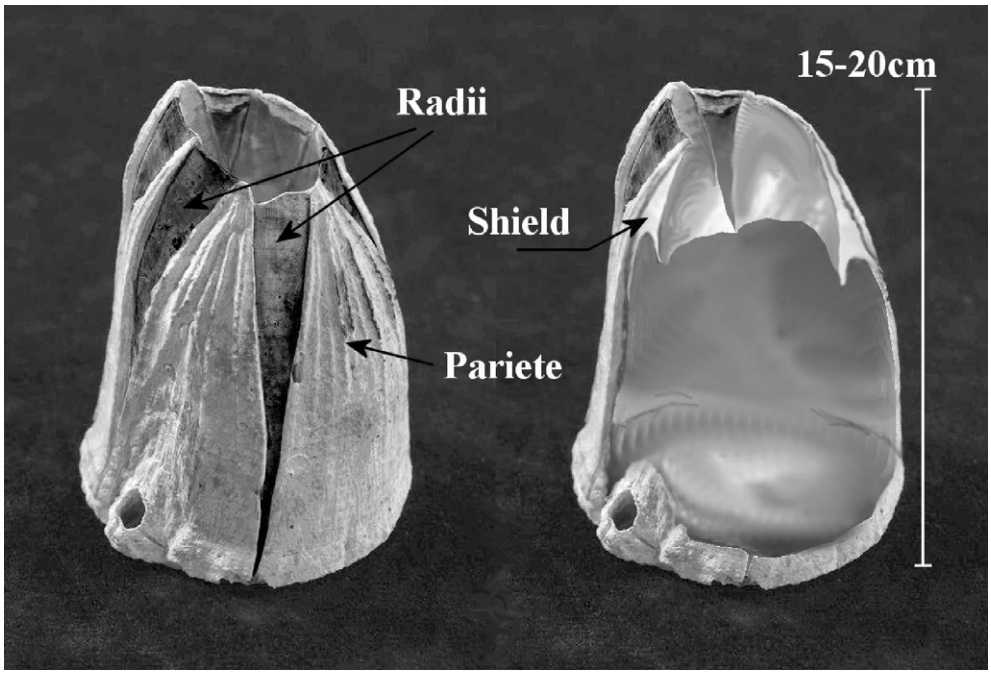

Fig. 1. Barnacle shell showing its different structural parts. (A) External shell (left), (B) Internal shell (right).

of the shell and build a quite stable and heavily mineralized wall made of a series of thick plates that completely surround the animal and are firmly cemented to the substratum. Thus, barnacle shell mineralization is quite different from other well studied systems (i.e., mollusk shell, eggshell). It is an interesting alternative model for studying biomineralization processes and deserves to be studied more intensively. Besides Darwin's pioneering studies (Darwin, 1854) and a few studies on barnacle's shell formation and structure (Bourget, 1977; Fernandez et al., 2001a,b), there is no detailed study of the organization of barnacle shell microstructure and the relationship between the organic matrix and the mineral. In this paper, we focus on the microstructure and crystallographic-texture of the barnacle shell to understand its formation and to determine which mechanisms control the development of its ordered microarchitectures. This study provides an insight into the influence of the organic matrix on shell mineral organization. The findings may also be applied to the fabrication of biomimetic materials, which are composed of highly oriented crystals of the same size and morphologies (Aksay et al., 1996). Also, this biomaterial could be of interest for biomedical applications as an alternative to nacre which has been successfully used in bone implants (Camprase et al., 1990; Atlan et al., 1997). In contrast to nacre, the barnacle shell contains calcite microcrystals (instead of aragonite microcrystals) and has considerable porosity (compared to nacre which is very dense material). The different composition and microstructural characteristics should affect dissolution behaviour in the body fluids (calcite being less soluble than aragonite) and porosity could favour bonding of this material with bone.

2. Materials and methods

2.1. Samples

Several shells from specimens of *Austromegabalanus psittacus* collected along in the coast of Chile were used for this study.

2.2. Optical and electron microscopy

The microstructure of different parts of barnacle shell was observed by optical (OM) and scanning electron microscopy (SEM). For transmitted-light microscopy, petrographic thin-sections (30 μm thick) of shell pieces cut along different orientations were prepared. SEM observation was carried out with both in fractured specimens and on the inner and outer of the different structural units of the shell. Samples were observed intact and after partially removing the organic material (with 5% sodium hypochlorite for 1–2 h at room temperature). Samples were coated with gold (Polaron E5000 sputtering) and observed using a variable-pressure SEM microscope (LEO 1430-VP, Germany).

2.3. Crystallographic-texture analysis

The three-dimensional orientation of the barnacle shells' crystals was determined using an X-ray single diffractometer equipped with an area detector (Bruker D8 SMART APEX, Germany). For diffraction experiments the working conditions were: Mo Kα, 50 KV and 30 mA, a pin-hole collimator of 0.5 mm in diameter and an exposure time of 20 s per frame. A set of frames (2-D diffraction patterns) was

registered while rotating the sample (typically, a small piece of shell of about 0.25 cm^2) around ϕ angle (a frame every 2 degrees; 90 frames in total). Pole densities for strongest calcite reflections (102, 104, 006, 110, 113, 202, 108, and 116) were calculated and displayed in stereographic projection using a specially designed software (*XTexture*, to be described in detail elsewhere). Each pole figure displays the intensity variation of a given *hkl* reflection as a function of the sample orientation. Sample orientation is defined by two polar angles, ϕ (rotation angle around the sample normal) and ψ (tilting angle of sample normal). From these plots, the 3-D orientation of direction normal to {*hkl*} crystal faces (or poles) can be observed. The scattering or degree of preferential orientation of the main crystal directions was quantified as the full width at the half maximum (FWHM) values of the peaks displayed in different pole figures. The lower the FWHM value measured in a *hkl* pole figure, the greater is the alignment of crystals along a given [*hkl*] crystallographic direction. To describe the orientation of crystals in the shell, pole figures in different structural parts were registered. To study the evolution of the orientation of crystals during shell growth, frames from different locations within the same structural unit were registered. From these frames, the spread in the tilting of specific crystal directions can be measured.

Additionally, the mineral phase of the shell material, crystal orientation and crystallite size (which is also a measure of crystallinity) were determined from θ–2θ scans using a powder diffractometer (Phillips PWD 1700, Holland; Rigaku Multiflex, Japan). The crystallite size was determined from 104 calcite reflections after applying the Scherrer equation (Cullity, 1977).

2.4. Chemical analyses

Organic matter and Mg content in different structural parts were determined by thermo gravimetric analyses (Shimadzu TGA-50H, Japan) and atomic absorption (Perkin Elmer AA-5100, USA), respectively.

3. Results

3.1. Microstructure of shell

Optical microscopy observation of longitudinal sections of a parietes reveals that this structural unit is constituted by an outer lamina which has a massive microstructure constituted by randomly oriented calcite microcrystals (Fig. 2A) and an inner lamina made by mineral layers (about 20 μm thick) separated by thin organic sheets (Fig. 2B). These mineral layers are composed of equiaxial calcite microcrystals. Under cross-polarized light, crystals making each mineral layer extinguish simultaneously, which indicates a high degree of crystal orientation. It can be also observed that both structural units are not fully dense but quite porous. Fig. 2C show a transverse section of a parietes formed from an outer organic rich lamina with channels (running from the base to the cone apex) and a mineral layer with an arrangement resembling a bunch of grapes. Each grape-like unit branches from an organic matrix-rich central line crossing through the middle of the structure. Also, each grape-like unit is transected by a central line of organic material. Under cross-polarized light, crystals in these units displayed an undulant extinction.

When observed by SEM, the external surface of the parietes shows a surface with ripples running parallel to the cone base and spaced out about 40 μm apart. This surface consists of equiaxial subrounded calcite crystals with sizes ranging from 0.5 to 1 μm (Fig. 2D). Fig. 2E displays the longitudinal fracture of a radius, which consists of superimposed mineral layers (about 20 μm thick) of equiaxial microcrystals. These mineral layers are curved around channels that run parallel to the basal plane. Interestingly, the orientation of the calcite crystals in the mineral layers changes as the layers curves in such a way that they are always oriented with their *c*-axis perpendicular to the organic sheets separating these layers. Even though the mineral layers are separated by organic sheets, there is a continuity in the orientation of the crystals as we move from one layer to the next. Fig. 2F shows a transverse fractured sample of the parietes displaying a ridged topography which is the same as that observed in the optical photomicrograph of Fig. 2C. The arrangement of crystals constituting this corrugated surface causes the undulant extinction observed for this structure under cross-polarized light. The inner shell surface is made up of globular aggregates (with sizes ranging from 0.5 to 2 μm) of calcite nanocrystals (Fig. 2G).

A transverse fracture of the shell shield revealed that it consists of subparallel oriented lamellae which are in turn composed of equiaxial calcite crystals with average sizes of about 0.25 μm (Fig. 2H). Finally, Fig. 2I shows the outer surface of the basal cement disk that bonds the shell walls to the substratum. It is made up of equiaxial calcite microcrystals ranging from 0.5 to 1 μm in size and which in some cases display idiomorphic morphologies. This microstructure resembles that of the inner shell surface.

3.2. Crystal orientation studied by X-ray diffraction

The orientation of crystals in the different structural units comprising the barnacle shell was determined by registering θ–2θ scans and pole figures from those units.

The θ–2θ scan from the outer shell surface (either from the parietes or from radii) shows the same diffractogram as that from a randomly oriented calcite powder sample (Fig. 3A). Pole figures from individual calcite reflections from the outer surface of the shell show uniform distribution of intensity, confirming that crystals have a random orientation.

On the other hand, the θ–2θ scan from the inner shell surface shows only 006 and 108 reflections, indicating that crystals are oriented with their *c*-axis nearly perpendicular to the surface (Fig. 3B). Pole figures from the inner surface

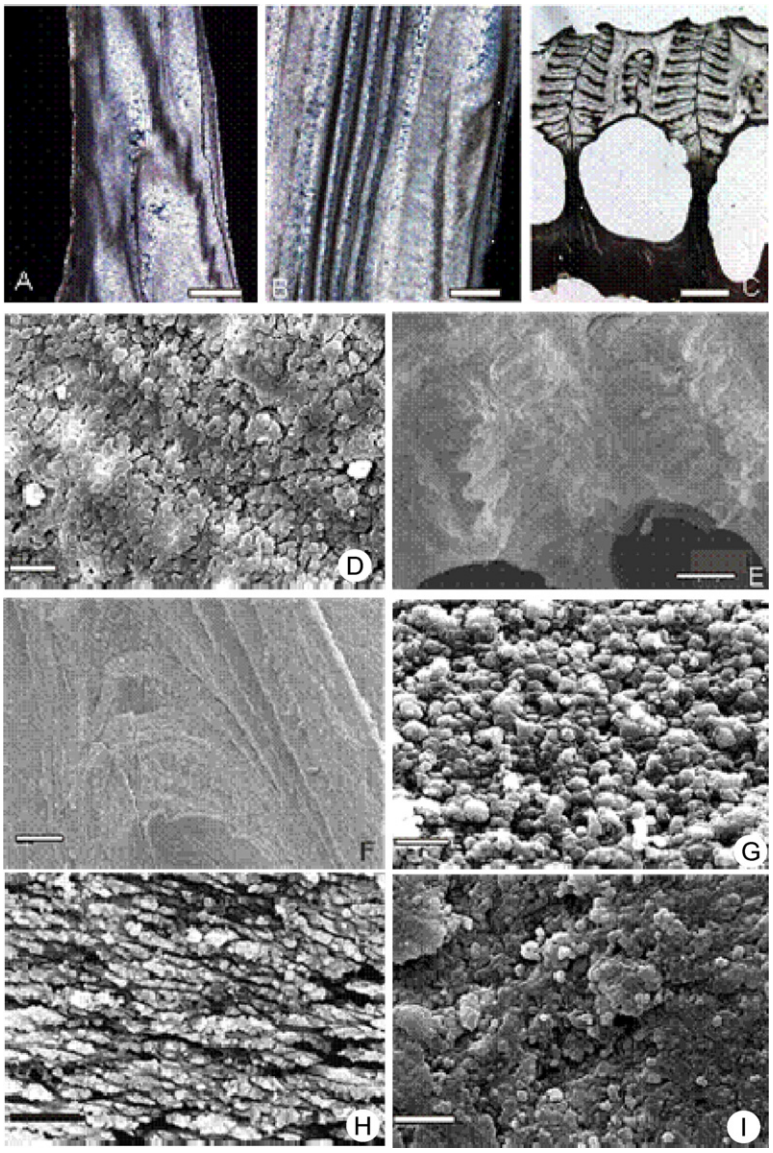

Fig. 2. (A) Photomicrograph of a longitudinal section of the pariete outer lamina as viewed under cross-polarized light. (B) Longitudinal section of the pariete internal lamina made of parallel mineral layers separated by thin organic sheets as viewed under cross-polarized light. (C) Transverse section from a pariete formed by an outer organic matrix-rich lamina separated by channels (running from the base to the cone apex) and a mineral-rich layer as viewed under parallel polarized light. (D) SEM Photomicrograph of the external surface of the parietes. (E) Longitudinal fracture of a radii formed by curved mineral layers around canals that run parallel to the basal plane. (G) Inner shell surface made of globular aggregates of calcite nanocrystals. (H) Transversal fracture of the shield formed by subparallel oriented lamellae. (I) Outer surface of the basal cement disk made up of equiaxial calcite microcrystals. Scale bars in (A, B, and C) 400 μm, (E) 200 μm, (F) 50 μm, and (D, G, H, and I) 5 μm.

of the shell show a non uniform distribution of intensity, indicating that crystals are non-randomly oriented. Specifically, 006 pole figures displayed a unique central maximum, indicating that crystals are aligned with their *c*-axis perpendicular to the shell surface. The breadth of this maximum (FWHM $\chi = 19.1°$) measures the spread of the orientation of the crystal *c*-axis. The 104 pole figure displays a ring of non uniform intensity. The separation angle between the ring and the centre of the pole figure at about 44° and corresponds to the interfacial angle between (0001) faces (normal to *c*-axis) and $(10\bar{1}4)$ faces (calcite rhombohedral faces). The breadth of the ring in χ angle displayed in 104 pole figure is in about the same (18°) as that of the maximum displayed in the 006 pole figure since related faces move together.

The θ–2θ scan from the external surface of the shell shield shows only 108 reflections, indicating that crystals are oriented with their *c*-axis nearly perpendicular to the surface (Fig. 4A). The 006 pole figure displays a single central maximum (with a FWHM $\chi = 17.4°$), indicating that crystals are aligned with the *c*-axis perpendicular to the shield outer surface but with slightly better orientation than in the shell inner surface. The 104 pole figure displays a ring with a very homogeneus intensity, indicating that crystals are rotated, one respect to another, around the *c*-axis (that is they have a turbostratic orientation).

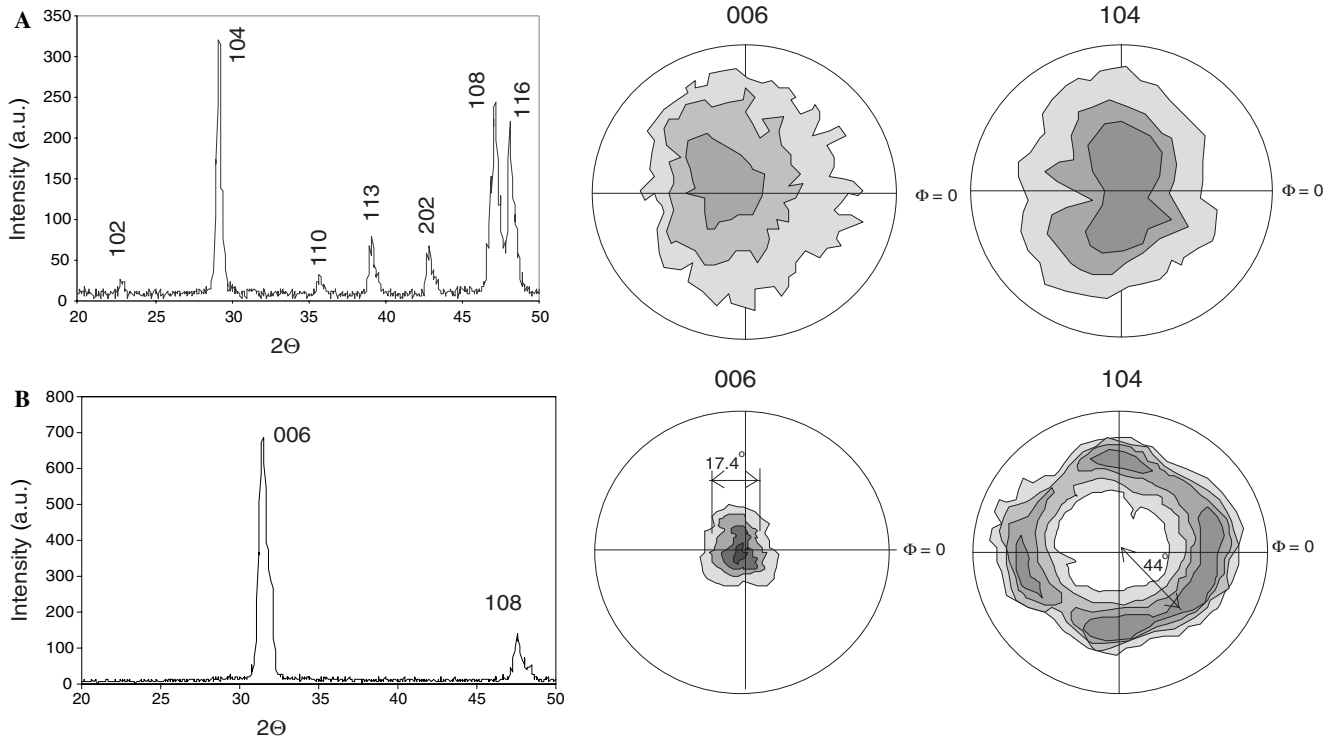

Fig. 3. (A) θ–2θ Scan from the outer shell surface showing a randomly oriented calcite powder pattern. The 006 and 104 pole figures show uniform distribution of intensity characteristic of the randomly oriented sample. (B) θ–2θ Scan from the inner shell surface showing only 006 and 108 reflections, indicating that crystals are oriented with their c-axis nearly perpendicular to the surface. The 006 pole figure displays an unique central maximum, indicating that crystals are aligned with their c-axis perpendicular to the shell surface. The 104 pole figure displays a ring of non uniform intensity.

On the other hand, the θ–2θ scan from the inner shield surface shows only reflections associated with calcite planes close or parallel to the c-axis (Fig. 4B). The intensities of these reflections are stronger than those in a randomly oriented calcite sample, especially when those planes are almost parallel to the c-axis. For instance, the most enhanced reflection is 110, associated with $(11\bar{2}0)$ planes which are parallel to the c-axis. That means the c-axis lies down parallel to the shell surface. However, to know the exact disposition of the crystals, it is necessary to study the pole figures of reflections. In this case, the 110 pole figure (describing the disposition of $[11\bar{2}0]$ directions which are perpendicular to the c-axis) is the most informative one. It displays an elongated maximum at 90 degrees from the shield growth direction. The breadth of this elongated maximum is about 19.5° (FWHM χ). This means that this direction lies in a plane perpendicular to the shield growth direction. This distribution confirms that the c-axis lies parallel to the shield inner surface. It also indicates that crystals have their c-axis aligned to the growth direction and are rotated, one respect to another, around the c-axis. Likewise, all other directions should be rotated around the c-axis. This is confirmed by the distribution of maxima in other pole figures. For example, the 104 pole figure displays two elongated maxima, with the elongation axis at 90 degrees from the growth direction. Each maximum is associated with the distribution of three $\{10\bar{1}4\}$ calcite faces either in the positive or the negative part of the c-axis. These two maxima are separated by about 83° which is approximately the interfacial angle between these two sets of faces. For clarity, Fig. 4C shows a calcite crystal oriented in the same way as that determined in the pole figures. In the same figure, the different types of faces and their directions are identified. Finally, note that the 006 pole figure should display two maxima, one at $\phi = 0°$ and $\chi = 90°$ and another at $\phi = 180°$ and $\chi = 90°$. However, the 006 pole figure does not display any maximum because of X-ray absorption which greatly reduces the reflected intensity at high tiling angles ($\chi > 60°$).

Crystals constituting the cement of the basal disk have a random orientation at the contact with the substratum while at the top surface they are preferentially oriented with their c-axis perpendicular to the cement surface (FWHM $\chi = 16.8°$) and are rotated around it ((001) fibre texture), similar to the orientation at the inner surface of the shell walls.

3.3. Evolution of the shell mineral crystallinity

Table 1 shows the organic matter, and Mg, contents and crystallite size in different structural parts of the barnacle shell. TGA analyses showed two marked weight loss events at around 300 and 470 °C, respectively, which can be attributed to organic matter combustion. Type A and type B refer to two different types of organic matter determined by TGA. Probably, type A is intercrystalline organic

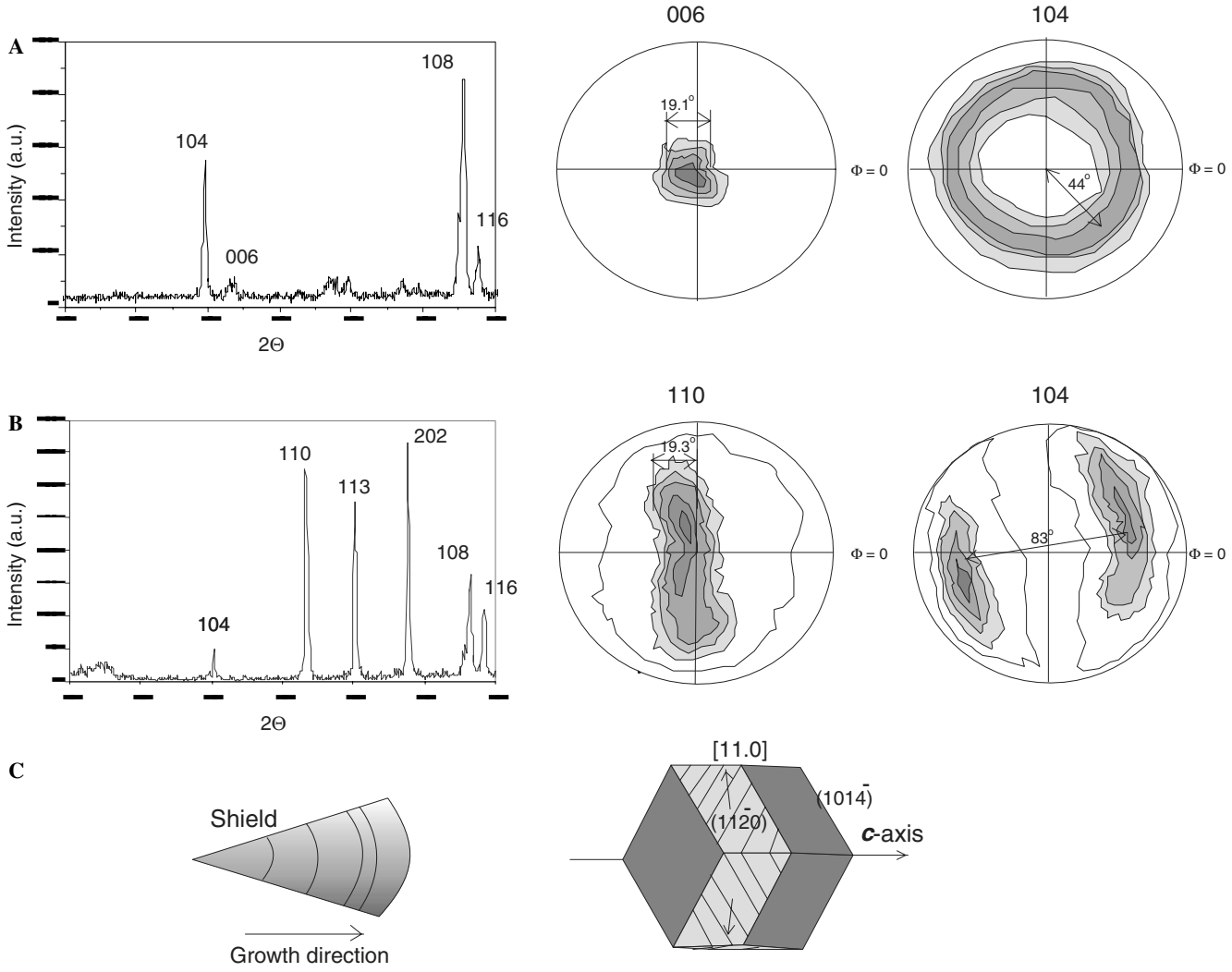

Fig. 4. (A) θ–2θ Scan from the external shield surface showing only 104, 006 and 108 reflections, indicating that crystals are oriented with their *c*-axis nearly perpendicular to the surface. The 006 pole figure displays a single maximum off-centered, indicating that crystals are aligned with the *c*-axis nearly perpendicular to the surface. The 104 pole figure displays a ring with very homogenous intensity, indicating that crystals are rotated, one respect to another, around the *c*-axis and have a (001) fibre texture. (B) θ–2θ Scan from the inner shield surface showing only reflections associated with calcite planes close or parallel to the *c*-axis, indicating that the *c*-axis lies down parallel to the shell surface. The 110 pole figure displays an elongated maximum at 90 degrees from the shield growth direction. The 104 pole figure displays two elongated maxima, with the elongation axis at 90 degrees to the growth direction. Each maximum is associated with the distribution of three $\{10\bar{1}4\}$ calcite faces either in the positive or the negative part of the *c*-axis. This distribution confirms that *c*-axis lies parallel to the shield inner surface and points parallel to the shell growth direction. (C) Schematic view of the shield and that of a calcite crystal oriented in the same way as that determined in the pole figures for calcite crystals making up this structural unit.

Table 1
Crystallite size in different location of barnacle shell determined using 104 calcite reflections (XRD) and applying Scherrer equation

Sample location	Cristallite size (nm)	Organic matter (%)		Mg (ppm)
		Type A	Type B	
Radii (*internal surface*)	49 ± 14	1.685	0.352	2879
Pariete (*internal surface*)	66 ± 24	1.144	0.428	2222
Radii (*external surface*)	67 ± 22	0.897	1.045	3000
Pariete (*external surface*)	80 ± 15	0.804	0.761	2193

Organic matter and Mg content were determined by TGA and AA, respectively.

matter and type B is intracrystalline organic matter. The former is typically lost at lower temperatures than the latter (Zaremba et al., 1998). In a cross section of the barnacle shell the sequence in which they appear (from inside to the outside) is approximately the following: (a) internal surface of the radii, (b) external surface of the radii, (c) internal surface of the parietes, and (d) external surface of the parietes. The separation between (b) and (c) faces is diffuse, but (a) and (d) are separated by approximately 4 mm. Interestingly, the crystallite size measured in the different structural parts of the barnacle shell decreases from the inner shell surface to the outer shell surface. In this sequence also the concentration of the organic matter (type B) in the shell increases. Thus, as the concentration of the specific organic components increases the crystallinity of

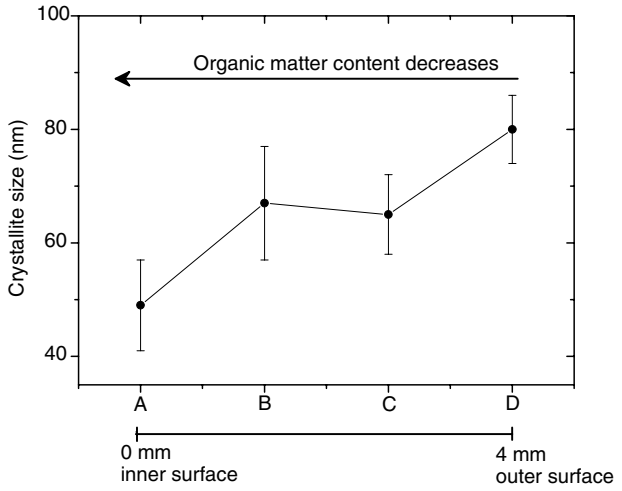

Fig. 5. Evolution of crystallite size (calculated using Scherrer equation) across the barnacle shell wall in relation to the organic matter content. A, B, C, and D correspond to the internal radii, internal pariete, external radii, and external pariete, respectively.

the shell mineral decreases. This trend is better visualized in Fig. 5. No relationship was observed between crystallite size and Mg content.

4. Discussion

The barnacle shell is made up of calcite microcrystals, which are arranged in various microstructure types in different parts of the shells. In the more external layer, the microcrystals are arranged in massive microstructures with no ordering. In layers toward the interior shell walls, crystals start to arrange in mineral layers separated by thin organic sheets, and the crystals a high degree of orientation. The evolution of the crystal arrangement during shell formation was studied by optical microscopy and crystallographic-texture analyses. The orientation of the crystals in the different layers of the shell walls evolves from randomly oriented (outer part) to an orientation with the *c*-axis aligned perpendicular to the shell walls (inner part) to the shell walls. The same type of transition occurred in the basal cement disk. The most drastic change in the orientation of the crystals occurred in the transition from the external to the internal surface of the shell shield where the orientation of the *c*-axis shifted from perpendicular to parallel to the shield surface and pointing parallel to the growth direction. These abrupt changes in the microstructure and crystallographic orientation of crystals is well described in molluscs, for which shells are commonly composed of superimposed layers containing a different microstructure and/or different type of $CaCO_3$ polymorph (Checa and Rodríguez-Navarro, 2005).

There is evidence from in vitro experiments that specific proteins, comprising the shell organic matrix, play an important role in controlling the polymorph type, size and morphology of precipitating crystals (Addadi and Weiner, 1992; Falini et al., 1995; Belcher et al., 1996). The major characteristics of barnacle shell mineral are very well defined. The shell mineral is composed of crystals of only one $CaCO_3$polymorph (calcite) of similar size (typically from 0.5 to 1 μm) and morphology (equiaxial). This suggests a high degree of control on the precipitation process by different components of the organic matrix. In fact, a previous study showed how organic components extracted from the barnacle shell greatly influence the precipitation of calcium carbonate, affecting the morphology, size and polymorphic phase of the mineral (Fernandez et al., 2001a,b). Barnacle shell organic matrix contains proteoglycans similar to those found in avian eggshell and mollusc shell organic matrix, which are very active in controlling the precipitation of calcium carbonate during the formation of these biomineral structures (Arias and Fernandez, 2001, 2003; Fernandez et al., 2001a,b, 2004; Levi-Kalisman et al., 2001; Arias et al., 2004).

On the other hand, the submicrometer size of calcite crystals forming different structural parts of the shell walls is much smaller than characteristic sizes of calcite crystals in other systems (mollusk shell and avian eggshell) which are at least few tens of micrometers (Checa and Rodríguez-Navarro, 2005; Rodríguez-Navarro et al., 2002). Some specific components of the organic matrix should be responsible for the reduced size of the crystals. For instance, Jimenez-Lopez et al. (2003) has shown that negatively charged proteins has an inhibitory effect on $CaCO_3$ precipitation and reduced the size of calcite crystals. This reduction in size could be induced by specific organic components of the shell organic matrix that promote a high flux of nucleation and which would result in the precipitation of a large number of crystals with very small sizes (Black et al., 1986; Lahav and Leiserowitz, 1993). It is worth noticing the negative correlation observed between the concentration of organic matter and calcite crystallite size (Fig. 5). Organic components can be preferentially incorporated into calcite crystals along specific crystal planes reducing the crystallite size in the direction perpendicular to these planes (Berman et al., 1993). Magnesium is known to affect calcite growth and morphology (Lippmann, 1973), however, no correlation was found between Mg content and crystallite size. Probably, Mg levels in the shell are too low to cause any notable effect.

It is also worth noticing the relationship between crystal orientation and the disposition of organic sheets separating the inner mineral layers. Calcite crystals were always oriented with their *c*-axis perpendicular to the organic sheets separating the mineral layers. This could be due to an oriented nucleation of calcite crystals on these organic sheets with their *c*-axis perpendicular to them. This is the most common orientation of calcite (and aragonite) in many different biomineral systems. It is caused by the accumulation of charged ions on the surface of the organic sheets (ionotropic effect Addadi et al., 1987), which favours the nucleation of calcite (or aragonite) with on their (001) basal planes that are composed by calcium ions. This oriented nucleation has been induced in vitro on substrates coated with acidic macromolecules (Addadi et al., 1987). Alternatively, the

preferential orientation of crystals could arise from a geometrical selection process as described in avian eggshells (Rodríguez-Navarro and García-Ruiz, 2000). On the other hand, the shift in the orientation *c*-axes from being perpendicular to the surface to being parallel observed, which in the shield is quite unusual and interesting. Similar transitions are observed in calcitic foliated layer in bivalves and in the walls of calcareous foraminifera (Taylor et al., 1969; Runnegar, 1984; Towe and Cifelli, 1969).

5. Conclusions

Barnacle shell structural units are mineralised by calcite microcrystals of very uniform size which are organised in a massive microstucture toward the external shell and in mineral layers separated by organic sheets toward the internal shell. There is a well defined relationship between the orientation of crystals and the disposition of organic sheets. Also, crystallite size is related to organic content in different structural parts. All these observations indicate that the organic matrix plays an important role in defining the organization of the shell mineral, exerting a strict control on the polymorphic type, size and orientation of shell forming crystals and to David A. Carrino (Case Western Reserve University) for correcting the manuscript.

Acknowledgments

This work was supported by FONDAP 11980002 granted by the Chilean Council for Science and Technology (CONICYT). A.R.N. acknowledge financial support through research grant REN2003-07375 and Programa Ramon y Cajal from the Spanish government. We also thanks J. Carrillo and J. Romero-Garzon (U. Granada) for technical assistance during SEM and XRD analyses.

References

Addadi, L., Moradian, J., Shay, E., Maroudas, N.G., Weiner, S., 1987. A chemical model for the cooperation of sulfates and carboxylates in calcite crystals formation. Proc. Natl. Acad. Sci. USA. 84, 2732–2736.

Addadi, L., Weiner, S., 1992. Control and design principles in biological mineralization. Angew. Chem., Int. Ed. Engl. 31, 153–169.

Aksay, I.A., Trau, M., Manne, S., Honma, I., Yao, N., Zhou, L., Fenter, P., Eisenberger, P.M., Gruner, S.M., 1996. Biomimetic pathways for assembling inorganic thin films. Science 273, 892–898.

Arias, J.L., Fernandez, M.S., 2001. Role of extracellular matriz molecules in shell formation and structure. Worlds Poult. Sci. J. 57, 349–357.

Arias, J.L., Fernandez, M.S., 2003. Biomimetic processes through the study of mineralizad shells. Mater. Charact. 50, 189–195.

Arias, J.I., 2002. Influence of different macromolecules present in matrices of natural bioceramics on in vitro calcium carbonate crystallization (in Spanish). Thesis DVM, Faculty of Veterinary and Animal Sciences, Universidad de Chile, Santiago, Chile, 40 pp.

Arias, J.L., Neira-Carrillo, A., Arias, J.I., Escobar, C., Bodero, M., David, M., Fernandez, M.S., 2004. Sulfated polymers in biological mineralization: a plausible source for bio-inspired engineering. J. Mater. Chem. 14, 2154–2160.

Atlan, G., Balmain, N., Berland, S., Vidal, B., Lopez, E., 1997. Reconstruction of human maxillary defects with nacre powder: histological evidence for bone regeneration. CR. Acad. Sci. Paris Life Sci. 320, 253–258.

Belcher, A.M., Wu, X.H., Christensen, R.J., Hansma, P.K., Stucky, G.D., Morse, D.E., 1996. Control of crystal phase switching and orientation by soluble mollusc-shell proteins. Nature 381, 56–58.

Berman, A., Hanson, J., Leiserowitz, L., Koetzle, Th.F., Weiner, S., Addadi, L., 1993. Biological control of crystal texture: a widespread strategy for adapting crystal properties to function. Science 259, 776–779.

Black, S.N., Davey, R.J., Halcrow, M., 1986. The kinetics of crystal growth in the presence of tailor-made additives. J. Crystal Growth 79, 765–774.

Bourget, E., 1977. Shell structure of sessile barnacles. Nat. Canadien 104, 281–323.

Camprase, S., Camprase, G., Pouzol, M., Lopez, E., 1990. Artificial dental root made of natural calcium carbonate (Bioracine). Clin. Mater. 5, 235–250.

Checa, A., Rodríguez-Navarro, A.B., 2005. Self-organisation of nacre in the shells of Pterioida (Bivalvia: Mollusca). Biomaterials 26, 1071–1079.

Cullity, B.D., 1977. Elements of X-ray diffraction. Addison-Wesley, Reading, MA, pp. 127–131..

Darwin, C., 1854. A monograph on the sub-class cirripedia. Ray Society, London.

Falini, G., Albeck, S., Weiner, S., Addadi, L., 1995. Control of aragonite or calcite polymorphism by Mollusk shell macromolecules. Science 271, 67–69.

Fernandez, M.S., Vergara, I., Oyarzún, A., Arias, J.I., Rodríguez, R., Wiff, J.P., Fuenzalida, V.M., Arias, J.L., 2001a. Extracellular matrix molecules involved in barnacle shell mineralization. Mat. Res. Soc. Symp. Proc. 724, 3–9.

Fernandez, M.S., Moya, A., Lopez, L., Arias, J.L., 2001b. Secretion pattern, ultrastructural localization and function of extracellular matriz molecules evolved in eggshell formation. Matrix Biol. 19, 793–803.

Fernandez, M.S., Passalacqua, K., Arias, J.I., Arias, J.L., 2004. Partial biomimetic reconstitution of avian eggshell formation. J. Struct. Biol. 148, 1–10.

Jimenez-Lopez, C., Rodríguez-Navarro, A., Domingez-Vera, J.M., Garcia-Ruiz, J.M., 2003. Influence of lysozyme on the precipitation of calcium carbonate. Kinetic and morphological study. Geochimica et Cosmochimica Acta 67, 1667–1676.

Lahav, M., Leiserowitz, L., 1993. Tailor-made auxiliaries for the control of nucleation, growth and dissolution of 2-dimensional and 3-dimensional crystals. J. Phys. D. 26, B22–B31.

Levi-Kalisman, Y., Falini, G., Addadi, L., Weiner, S., 2001. Structure of the nacreous organic matrix of a bivalve mollusc shell examined in the hydrated state using cryo-TEM. J. Struct. Biol. 135, 8–17.

Lippmann, F., 1973. Sedimentary carbonate minerals. Springer, Berlin.

Lowenstam, H.A., Weiner, S., 1989. On Biomineralization. Oxford University press, New York, pp. 111–122..

Nousek, N.A., 1984. Shell formation and calcium transport in the barnacle *Chthamalus-fragilis*. Tissue Cell 16, 433–442.

Rodríguez-Navarro, A., García-Ruiz, J.M., 2000. Model of textural development of layered aggregates. Eur. J. Mineral 12, 609–614.

Rodríguez-Navarro, A., Kalin, O., Nys, Y., García-Ruiz, J.M., 2002. Influence of the microstructure on the shell strength of eggs laid by hens of different ages. British Poultry Science 43, 395–403.

Runnegar, B., 1984. Crystallography of the foliated calcite shell layers of bivalve molluscs. Alcheringa 8, 273–290.

Taylor, J.D., Kennedy, W.J., Hall, A., 1969. Shell structure and mineralogy of the Bivalvia. Introduction. Nuculacae–Trigonacae. Bull. Br. Museum Nat. Hist. Zool. 3 (Suppl.), 1–125.

Towe, K.W., Cifelli, R., 1969. Wall ultrastructure in the calcareous faraminifera: crystallographic aspects and a model for calcification. J. Paleontology 41, 742–762.

Zaremba, C.M., Morse, D.E., Mann, S., Hansma, P.K., Stucky, G.D., 1998. Aragonite-hydroxyapatite conversion in gastropod (abalone) nacre. Chem. Mater. 10, 3813–3824.